



Full Text View

[Volume 29, Issue 8 \(August 1999\)](#)

Journal of Physical Oceanography

 Article: pp. 2050–2064 | [Abstract](#) | [PDF \(341K\)](#)

The Origin of an Anomalous Ring in the Southeast Atlantic

Elaine L. McDonagh and Karen J. Heywood

School of Environmental Sciences, University of East Anglia, Norwich, Norfolk, United Kingdom

(Manuscript received December 1, 1997, in final form July 31, 1998)

DOI: 10.1175/1520-0485(1999)029<2050:TOOAAAR>2.0.CO;2

ABSTRACT

A warm core ring in the southeast Atlantic, previously thought to have come from the Brazil–Falklands (Malvinas) confluence, is traced back to the Agulhas retroflection. The path of this ring, sampled at 36°S, 4°E on 23 January 1993 during the World Ocean Circulation Experiment one-time hydrographic section A11, is resolved using a combination of satellite altimeter data from *ERS-1* and TOPEX/POSEIDON and infrared radiometer data from *ERS-1*'s Along Track Scanning Radiometer (ATSR). The *ERS-1* 35-day repeat and the TOPEX/POSEIDON 10-day repeat altimeter-derived sea surface height anomalies are combined and used to trace the ring back to 40°S, 10°E at the beginning of the *ERS-1* 35-day repeat mission in April 1992 when it had a sea surface height anomaly in excess of 50 cm. This anomaly in this part of the ocean is too large to be associated with a ring formed anywhere other than the Agulhas retroflection. The ring is identified in coincident 35-day altimetry fields and in a monthly average of ATSR sea surface temperature data in August 1992. That this anomaly was observed in the ATSR data indicates that the ring has not overwintered; the age and speed since formation inferred from this precludes formation outside of the Agulhas retroflection region. Using ATSR data prior to April 1992 and altimetry data from *ERS-1*'s 3-day repeat, this ring is traced back to the Agulhas retroflection where it formed in October 1991.

The ring was unlike any previously sampled ring in this region, as it had a homogeneous core between 100 and 550 db, potential temperature 13°C, salinity 35.2 psu and potential density 26.55. This water lay on the same potential temperature–salinity (θ – S) curve as the water within a typical Agulhas ring sampled a few days later. The peak velocity measured within the ring by an acoustic Doppler current profiler at 200 m was 58 cm s^{−1}. This velocity was similar to other Agulhas rings, but higher than the velocities measured in rings originating in the Brazil–Falklands (Malvinas) confluence region. The high oxygen and low nutrient concentrations (relative to typical Agulhas water) and θ – S characteristics of the core of the anomalous ring were consistent with a mode water that forms in the subantarctic zone of the southwest Indian Ocean, subantarctic mode

Table of Contents:

- [Introduction](#)
- [Hydrographic and remotely](#)
- [Tracing Ring 1 during](#)
- [Tracing Ring 1 in the](#)
- [Structure of the section](#)
- [Subantarctic mode water](#)
- [Paths of SAMW from its](#)
- [Discussion](#)
- [REFERENCES](#)
- [FIGURES](#)

Options:

- [Create Reference](#)
- [Email this Article](#)
- [Add to MyArchive](#)
- [Search AMS Glossary](#)

Search CrossRef for:

- [Articles Citing This Article](#)

Search Google Scholar for:

- [Elaine L. McDonagh](#)
- [Karen J. Heywood](#)

water (SAMW). The type of SAMW detected in the anomalous ring has been observed forming by deep convection in the subantarctic zone at 60°E. At this longitude water is readily subducted from the subantarctic zone into a pronounced and compact anticyclonic gyre in the western south Indian Ocean. A particle tracing experiment in the mean velocity field of the Fine Resolution Antarctic Model showed that it would take eight years (within a factor of 2) for water to recirculate from near 40°S, 60°E into the Agulhas retroflection in this compact gyre. Once in the retroflection, the SAMW is available to be pinched off into rings.

1. Introduction

The western boundary current of the south Indian Ocean subtropical gyre, the Agulhas Current, is still flowing poleward when it leaves the coast of South Africa. South of Africa it executes an abrupt anticyclonic turn (the Agulhas retroflection) and flows off eastward as the southern boundary of the south Indian Ocean subtropical gyre (the Agulhas Return Current). Occasionally, the Agulhas retroflection occludes and rings are pinched off. The frequency of this occlusion has been observed to vary between six and nine per year ([Feron et al. 1992](#); [Lutjeharms and van Ballegooyen 1988](#)). Approximately 30 of these rings have been observed at sea since the first in 1964 by [Duncan \(1968\)](#).

The elevated sea surface temperatures associated with Agulhas rings, relative to the South Atlantic water in which they are embedded, allows the rings to be detected using satellite sea surface temperature images ([Lutjeharms and van Ballegooyen 1988](#)). However, the sea surface temperature anomaly associated with Agulhas rings is eroded as they interact with the atmosphere and, once the rings overwinter, the surface temperature anomaly is completely destroyed. [Lutjeharms and van Ballegooyen \(1988\)](#) found no discernible sea surface temperature anomalies west of approximately 7°E or north of 33°S. Sea surface height data do not have this problem since the bulge in the sea surface persists as long as the warm core of the ring does. Mapped sea surface height anomaly data from the Geosat altimeter have been used to trace over 20 anticyclonic rings from the Agulhas retroflection across the South Atlantic as far as its western boundary at 40°W ([Byrne et al. 1995](#)).

Rings formed at the Agulhas retroflection contain upper-level water masses (i.e., intermediate, central, and surface waters). The primary source of these waters in the Agulhas retroflection is the south Indian Ocean. There is also some local modification of surface waters and some introduction of South Atlantic water. Typically, an Agulhas ring comprises the highly stratified central waters generally associated with the Agulhas retroflection and surface waters that have at least been partially modified by heat loss to the atmosphere. For a typical potential temperature–salinity (θ – S) plot of the Agulhas retroflection region see [Fig. 11a](#) in [Gordon et al. \(1987\)](#). These rings facilitate a positive flux of heat, salt, and volume from the south Indian to the South Atlantic Ocean. This flux contributes to the upper-level return flow of the thermohaline circulation. Although the significance of Agulhas rings as part of the thermohaline circulation is not doubted, the magnitude of their contribution is still very much a topic of debate ([Macdonald and Wunsch 1996](#); [Schmitz 1995](#); [Gordon et al. 1992](#)).

Anticyclonic rings observed in the southeast Atlantic Ocean have generally been considered to have formed at the Agulhas retroflection. During 1993 there were three sightings of two rings in the southeast Atlantic, which were apparently different from the Agulhas rings previously sampled in this region. The most marked difference was the thick homogeneous core with higher oxygen and lower nutrient concentrations than is typically seen in the stratified Indian Ocean thermocline water. [Smythe-Wright et al. \(1996\)](#) and [Duncombe Rae et al. \(1996\)](#) concluded that these two anomalous rings had formed at the Brazil–Falklands (Malvinas) confluence region, and travelled across the South Atlantic in the southern limb of the subtropical gyre. These conclusions were based on hydrographic and tracer chemistry data. Determining the origin of these two anomalous rings allows the fluxes they facilitated to be categorized as either intraocean or, perhaps more importantly, interocean fluxes, which contribute to the warm water return path of the thermohaline circulation.

The WOCE one-time hydrographic section, A11 (cruise number D199), was occupied between 22 December 1992 and 1 February 1993 on RRS *Discovery* ([Saunders et al. 1993](#), [Fig. 1](#)). In the Cape Basin two warm core rings were encountered. The first of these was one of the anomalous rings sampled that year (hereafter Ring 1). The second feature (hereafter Ring 2), traversed two days later, was without doubt an Agulhas ring. Between these two features was a frontal jet. The objective of this study was to determine the origin of Ring 1, both where the ring itself formed and where the water that made up the core of the ring formed. Both sea surface temperature and sea surface height data (discussed in [section 2](#)) from satellites were used to trace Ring 1 (eddy B in [Smythe-Wright et al. 1996](#); eddy B2-1 in [Duncombe Rae et al. 1996](#)) from where it was observed in the Cape Basin to its region of genesis ([sections 3](#) and [4](#)). It will be demonstrated that contrary to the findings of [Smythe-Wright et al. \(1996\)](#), Ring 1 originated at the Agulhas retroflection. The structure of the A11 section ([section 5](#)) will be compared to the sources of the Agulhas Current ([sections 6](#) and [7](#)) to determine how this anomaly might have occurred and where the water at the core of Ring 1 originated.

2. Hydrographic and remotely sensed data

The principal instrument employed for the A11 hydrographic section (Fig. 1) was a Neil Brown Instrument Systems Mk IIIb Conductivity–Temperature–Depth Probe (CTD) fitted with a SensorMedic oxygen sensor and a General Oceanics rosette equipped with twenty-four 10-L Niskin water sample bottles. Additional data were obtained from expendable bathythermographs (XBTs). The horizontal density of salinity data was improved by merging salinity onto the XBT temperature profiles using the temperature–salinity relationship from an appropriate CTD station.

Data from the hull-mounted RD Instruments 150-kHz Acoustic Doppler Current Profiler (ADCP) were also used. These ADCP data for A11 have previously been described by [Saunders and King \(1995\)](#). Using a three-dimensional Global Positioning Satellite system the data are accurate to 1 cm s^{-1} when steaming between CTD stations. ADCP data shown here have been averaged over ten minutes and then smoothed using a running mean filter of length 110 min (equivalent to approximately 40 km when the ship is steaming).

When Ring 1 was sampled in situ, two satellites with onboard altimeters were operational, *ERS-I* and TOPEX/POSEIDON (T/P). Data from the *ERS-I* onboard infrared radiometer (Along Track Scanning Radiometer; ATSR) were also used. *ERS-I* had been orbiting in a 35-day repeat since 14 April 1992. Prior to this, *ERS-I* was in a 3-day repeat orbit since its launch in July 1991. TOPEX/POSEIDON had flown in a 10-day repeat orbit since 23 September 1992. The availability of coincident data from more than one altimeter offers the opportunity of more accurate ring tracing through increased data acquisition. At 35°S , adjacent parallel ground tracks are separated by approximately 260 km for T/P, 65 km for the *ERS-I* 35-day repeat, and 760 km for the *ERS-I* 3-day repeat. Rings previously sampled by Geosat data in this region have typical diameters of 250 km (defined by the extent of the positive sea surface height anomaly; [van Ballegooyen et al. 1994](#)). Therefore *ERS-I*, in its 35-day repeat orbit, is the only altimeter mission assured of even sampling, let alone resolving, the anomaly associated with an Agulhas ring. A study of mesoscale variability in the Azores region found that the *ERS-I* 35-day repeat data better described the mesoscale field than the T/P data alone ([Hernandez et al. 1995](#)), and showed a further improvement by combining data from the altimeters.

Both the *ERS-I* and T/P data were corrected for dry and wet tropospheric effects, ionospheric effects, the inverse barometer effect, sea state bias, and tides. Ocean and load tides were corrected using the [Cartwright and Ray \(1990\)](#) model. The data were then collocated onto a 7-km alongtrack grid. A tilt-bias technique, based on that of [Cheney et al. \(1983\)](#), was applied to remove the remaining orbit error. The length of the ground tracks made it necessary to remove an additional quadratic curve from the alongtrack data to further reduce orbit errors. The data were then smoothed alongtrack using a 30-km running median and a 30-km running mean filter.

To fully exploit the high across-track spatial resolution of the *ERS-I* 35-day repeat orbit, 35-day fields of sea surface height anomaly data were constructed. These fields were based on the 18 repeat cycles of *ERS-I* between April 1992 and December 1993.

After September 1992, data from the T/P altimeters were available and were combined with the *ERS-I* data in the fields. Over 35 days, a ring travelling at 5 cm s^{-1} would move approximately 150 km, or approximately one ring diameter, so a sea surface height anomaly would be smeared over a maximum of two ring diameters. Each of these fields therefore utilized the fine spatial resolution of the *ERS-I* 35-day repeat without making the temporal resolution so coarse that the anomaly associated with the ring was unidentifiable as such.

Sea surface height anomaly data, from the *ERS-I* and T/P altimeters, in the region 50°S to 20°S , 10°W to 20°E for each 35-day period were interpolated onto a 0.2° by 0.2° grid using a weighted average based on the inverse square of the distance, with a search radius of up to 0.3° (Fig. 2). The grid was fine enough to retain some of the high along-track resolution while the search radius was small enough to limit interpolation and capitalize on the high across-track resolution of the *ERS-I* data. The search radius was chosen so that data were interpolated across the diamond shaped gaps between the *ERS-I* ground tracks ($\sim 65 \text{ km}$) but not across large areas of data drop out or the diamonds between the T/P ground tracks ($\sim 260 \text{ km}$).

As a result of cloud cover, individual images from the *ERS-I* ATSR rarely showed a coherent picture. Therefore ATSR data were averaged into month-long fields and interpolated onto a 0.5° by 0.5° grid. An additional correction was made to the ATSR data to eliminate contamination problems due to nighttime cloud ([Jones et al. 1996](#)). Sea surface temperature data from NOAA's Advanced Very High Resolution Radiometer (AVHRR) were also studied, but suffered from more data gaps due to cloud contamination than the ATSR data, so will not be discussed further.

3. Tracing Ring 1 during the *ERS-I* 35-day repeat

A sea surface height anomaly profile was constructed by interpolating the gridded field (described in [section 2, Fig. 2a](#)) coincident in time with the cruise onto a line coincident with the cruise track. Values were calculated for points spaced 35 km apart along this line to simulate the average spacing between XBT and CTD stations. [Figure 3](#) shows this sea surface height anomaly profile and, for comparison, a profile of dynamic height at 100 db relative to 760 db calculated from

CTD and XBT profiles. The 35-day field of sea surface height anomaly reproduced well the major features seen in the dynamic height. Positive sea surface height anomalies of about 10 cm were associated with both rings, approximately one half and one third of the anomalies in dynamic height for Ring 1 and Ring 2, respectively. It was to be expected that the altimeter would underestimate the height anomaly associated with the rings. This is due to smoothing of the data during processing, interpolation, and because the altimeter ground track may not cross the center of the ring. Differences between the two fields will also arise from the dynamic height neglecting the barotropic component of the flow and assuming a level of no motion at 760 db.

Ring 1 and Ring 2 were both evident in cycle 8 (Fig. 2b), which ended only a week before the two rings were sampled on A11. The anomalies associated with Ring 1 (37°S, 4°E) and Ring 2 (34°S, 11°E) in cycle 8 were slightly to the southeast of the cruise track, which implies a northwestward movement of the rings during cycles 8 and 9. Ring 1 was easily traced backward in time to cycle 1, April 1992 (Fig. 2i). Ring 2, seen at approximately 34°S, 11°E in cycle 8, was not discernible in cycle 7 as it was almost certainly passing through the region of high variability associated with the Agulhas retroflection. The path of Ring 2 through this highly variable region is confirmed by Goni et al. (1997); Ring E2-92 in their Fig. 5a).

During August 1992 the position of Ring 1 deduced from the altimetry data was associated with a local maximum of approximately 12.5°–13°C in sea surface temperature (Fig. 4). This was a positive anomaly of 1°–2°C over the general meridional gradient in temperature. The movement of the ring, as well as the averaging and gridding of the ATSR data (described in section 2), caused the anomaly to become smeared. Discerning the spatial extent and magnitude of the temperature anomaly was therefore difficult. Nevertheless the month-long field contained an anomaly that was discrete enough (contained within two diameters of the ring) and large enough (greater than the precision of the sensor, $\pm 0.5^\circ$ C; Forrester and Challenor 1995) to be considered a real anomaly associated with Ring 1. Radiometer data studied for the months after August 1992 until January 1993 when Ring 1 was sampled in situ showed no such temperature anomaly associated with the altimeter-derived position of Ring 1. Cooling at the end of the 1992 winter must have destroyed the surface temperature signal associated with the ring. The correlation of the altimetry and ATSR datasets in the region of Ring 1 in August 1992 validated the use of monthly averages of sea surface temperature from the ATSR as a tool to trace the ring prior to September 1992.

4. Tracing Ring 1 in the ERS-1 3-day repeat

Tracing a ring using altimetry data from a 3-day repeat orbit is fundamentally different to tracing a ring sampled by an altimeter in a 35-day repeat orbit. The space between the 3-day repeat tracks (~ 760 km) is large compared to the diameter of the ring, and therefore mapping such data would either leave enormous gaps or require so much interpolation as to obliterate the alongtrack mesoscale signal. Successfully using the 3-day repeat data to trace a ring requires the ring to be beneath one of the widely spaced ground tracks. Supplementary information such as that from satellite radiometry was therefore required to conclusively trace the ring backward, particularly in the space between the 3-day repeat ground tracks.

The anomaly associated with Ring 1 was first observed in the 35-day repeat altimetry data at 40°S, 10°E in April 1992. In early March and February 1992 Ring 1 was detected by the ERS-1 altimeter in its 3-day repeat ice phase. Ring 1 moved across track 22 (Fig. 5b) with a maximum positive anomaly of 40 cm at a latitude of 41°S (Fig. 5a), consistent with the position of Ring 1 in the March 1992 ATSR picture. As the sea surface height anomalies for each repeat sampling of the ring were all at approximately one latitude, Ring 1 must have moved on a path almost perpendicular to the ground track (i.e., it had no alongtrack component of translational velocity). As a 3-month mean was used in the calculation of these sea surface anomaly data, the magnitude of this anomaly may be underestimated by 50% (McDonagh 1997). The effect of using a 3-month mean was evident in the repeat tracks preceding and subsequent to Ring 1 being sampled, as negative anomalies of up to 40 cm were recorded. The earliest sighting of Ring 1 in the 3-day repeat commissioning phase altimetry data (Fig. 5c) was along track 22 (Fig. 5d) in October 1991. The ring was spawned at the Agulhas retroflection region in October 1991 at 40°S. Ring 1 was evident moving southward down this track during November and the beginning of December 1991 when the commissioning phase ended.

Using a combination of altimeter (T/P and ERS-1 35 and 3 day repeats) and radiometer (ATSR) data it was possible to trace Ring 1 back to its point of genesis at the Agulhas retroflection. The path of Ring 1 from October 1991, when it was formed at the Agulhas retroflection to January 1993 when it was sampled on WOCE Cruise A11, is represented by monthly positions in Fig. 1.

5. Structure of the section

Potential temperature, salinity, and potential density sections showed that the core of Ring 1 was homogeneous, and the core of Ring 2 was highly stratified (Fig. 6). The North Subtropical Front was evident in these sections as steeply sloping isopleths at 5.5°E. The core pycnostad of $\sigma_\theta = 26.55$ associated with Ring 1 lay between 100 and 550 db and had a potential temperature of 13°C and a salinity of 35.2 psu. Above 200 db the isopycnals were domed, causing a reversal in the

geostrophic shear that resulted in a reduction in anticyclonic velocity. The maximum velocity of 58 cm s^{-1} within Ring 1 was seen at a depth of 200 m, whereas within Ring 2 the velocity increased from 60 cm s^{-1} at 200 m (Fig. 7) to a surface maximum of 92 cm s^{-1} . The erosion of the surface structure of Ring 1 and subsequent subsurface maximum in azimuthal velocity was caused by the ring overwintering since formation and its associated interaction with the atmosphere.

The core of Ring 1 (the cluster of points at $\theta = 13^\circ\text{C}$, $S = 35.2 \text{ psu}$) lay on the same θ - S curve as the stratified water within Ring 2 (Fig. 8). Therefore, in θ - S space Ring 1 was not cooler and fresher than a typical Agulhas ring (Ring 2), as was speculated in the cruise report (Saunders et al. 1993) and stated by Smythe-Wright et al. (1996). The South Indian Central Water (SICW) within the rings followed a very similar curve to the South Atlantic Central Water (SACW) outside the rings. However, within Ring 2 the SICW was approximately 0.1 more saline at any given potential temperature between 11° and 14°C than the water in which it was embedded. The homogeneous core of Ring 1 at $\theta = 13^\circ\text{C}$, $S = 35.2 \text{ psu}$ was also more saline than the SACW, but below the core the θ - S curve for the CTD data within Ring 1 relaxed (at around 11° – 12°C) to the same curve as the SACW (Fig. 8).

The core of Ring 1 had higher dissolved oxygen concentrations and lower nutrient concentrations than the water at the core of Ring 2 (Fig. 9). It was a combination of the anomalous nutrient and oxygen concentrations, and the not so anomalous θ - S characteristics of Ring 1 when compared with Ring 2, that led Smythe-Wright et al. (1996) to conclude that Ring 1 could not have an eastern Atlantic origin. However, both the θ - S properties and oxygen and nutrient concentrations in Ring 1 are consistent with a mode water that is a constituent of SICW, and therefore within the source water of the Agulhas retroflection. This is subantarctic mode water (SAMW).

6. Subantarctic mode water in the southwest Indian Ocean

During the Agulhas Retroflection Cruise (ARC) in late 1983, a pycnostad of 13.6°C was observed between depths of 600 and 725 m at CTD station 60 (hereafter ARC60) within the main retroflection (Gordon et al. 1987). The oxygen and nutrient concentrations at the potential temperature associated with that pycnostad were consistent with the water within Ring 1 (Fig. 9). Even in the typical Agulhas ring, Ring 2 (Fig. 9), there was a kink toward higher oxygen concentrations at around 13°C , and a coincident kink to lower nutrient (particularly silicate) concentrations. This implies that some of this mode water was present within Ring 2.

Gordon et al. (1987) and Fine et al. (1988) used data from the ARC to ascertain the origin of the water in the Agulhas retroflection. These studies provided compelling evidence that the ARC60 pycnostad ($\sigma_\theta = 26.55$) originated in the Indian Ocean rather than the South Atlantic. Gordon et al. (1987) compared the water within the retroflection with the inflow to the retroflection to assess the effect of local modification and mixing with South Atlantic water on the thermohaline structure of the Indian Ocean input. Using the method of Gordon and Haxby (1990) and a one-month residence time for water in the retroflection, an average net heat flux in excess of 2500 W m^{-2} from the ocean would be required to convert the input to the retroflection (ARC stations 49 and 50) to a 13.6°C thermostad. This heat flux is unfeasibly large, and greatly in excess of the 300 W m^{-2} estimated by van Ballegooyen et al. (1994) from Agulhas rings during the Subtropical Convergence and Retroflection Cruise (SCARC). The SCARC net heat fluxes are the largest reported for the Agulhas retroflection region. This is partly due to enhanced conditions for turbulent heat fluxes from the ocean during SCARC (Mey et al. 1990). Therefore the stad was almost certainly not formed by surface modification in the retroflection. The effect of mixing South Atlantic water into the Agulhas retroflection reduced the salinity of the water within the retroflection relative to the inflow, which was described as a negative salinity anomaly by Gordon et al. (1987). The stad at ARC60 was not discussed at length by Gordon et al. (1987), but was noted for having a positive salinity anomaly relative to the inflow, implying that the water definitely came from the south Indian Ocean rather than the South Atlantic. This point was reinforced by the work of Fine et al. (1988) using the same ARC data. They concluded that at the time of the ARC at least 23% of the Agulhas retroflection outflow was South Atlantic water that had mixed into the Indian Ocean. The mixing of South Atlantic water was not homogeneous throughout the water column. The Indian sector SAMW ($\sigma_\theta = 26.610$) was the water mass least affected by South Atlantic input in the retroflection and was well preserved in the outflow from the retroflection. This would lead one to conclude that the ARC60 mode water at $\sigma_\theta = 26.55$ was Indian Ocean in origin, and further imply that the mode water of the same density in Ring 1 also formed in the Indian Ocean.

Although the pycnostad at ARC60 was not identified as Indian Ocean SAMW by Gordon et al. (1987) and Fine et al. (1988), it seems very likely that it was SAMW that had recirculated into the retroflection. SAMW was first reported under this name by McCartney (1977). Southern Ocean wintertime data revealed deep (400–600 m) well-mixed layers immediately north of the Circumpolar Subantarctic Front. Heating during spring and summer isolated these layers from the surface, but did not erase them. McCartney (1977) found that the thermostad associated with SAMW could be traced as far north as the South Equatorial Current regions of each Southern Hemisphere subtropical gyre.

To ascertain the spatial distribution and temperature of deep mixed layers such as those associated with SAMW

formation, mixed layer depths were calculated using a 0.5°C criterion from the World Ocean Atlas (WOA94) objectively analyzed seasonal temperature fields on a one-degree grid. In the south Indian Ocean there is a band of deep wintertime convection that spans 35°S to 50°S with temperatures between approximately 8° and 13°C (Fig. 10), consistent with McCartney's (1977) description of the SAMW formation zone; deep mixed layers, which become cooler, fresher, and more dense toward the east. Two stations that measured deep convection in the southwest Indian Ocean were found in the WOA94 database, sampled by the Anton Bruun (AB) in September 1963 at 40.9°S, 60°E and 38.4°S, 59.9°E. One of these stations was used by McCartney (1977) in his definition of SAMW. The SAMW sampled by the AB was represented by a cluster of points at $\sigma_\theta = 26.6$ (Fig. 11). The homogeneous layer stretched from the surface to 500-m depth and was undoubtedly the product of deep winter convection. The two stations, which were 300 km apart, showed potential temperature, salinity, oxygen, and nutrient concentrations consistent with the core properties of Ring 1 and the pycnostad of ARC60 (Fig. 9).

The type of SAMW more usually detected in the Agulhas retroflection (10° to 12°C; Gordon et al. 1987; Duncombe Rae 1991) is cooler than the type sampled by the AB and at ARC60 (~13°C) and is, therefore, formed farther east in the south Indian Ocean. Figure 10 shows that the deep convection that forms SAMW is more widespread in the southeast Indian Ocean than in the southwest and central areas, so more of this cooler water feeds into the subtropical gyre (McCartney 1982) and ultimately the Agulhas retroflection. For the ~13°C SAMW observed by the AB at 60°E to enter the Agulhas retroflection, where it was observed at ARC60, there must have been some anomaly in, or enhancement of, mode water formation and/or circulation.

7. Paths of SAMW from its formation region to the Agulhas retroflection

Chlorofluorocarbon (CFC) data from 32°S in the Indian Ocean show that the most recently ventilated SAMW in the subtropics is found west of 72°E (Fine 1993). This implies that not only is there a mechanism in place to subduct SAMW from the subantarctic to the subtropics, but also that this mechanism is strongest west of 72°E. These recently ventilated subantarctic waters enter a pronounced and compact anticyclonic gyre in the southwest Indian Ocean. Although evidence for such a subgyre has existed in the literature for some time, only recently have the historical data been compiled to characterize the flow (Stramma and Lutjeharms 1997). They concluded that in the top 1000 m most of the recirculation associated with the south Indian Ocean subtropical gyre occurs in the western and central parts of the basin. Therefore if the mechanism to subduct SAMW into the subtropics is in place in the southwest Indian Ocean (Fine 1993) and the circulation to transport this water into the retroflection is also in place (Stramma and Lutjeharms 1997), then the limiting factor for 13°C SAMW reaching the retroflection is its formation rate in the subantarctic. The AB observations of SAMW forming as far north as 38.4°S were farther north than the mean location of the subtropical front (STF: approximately 42°S around the 60°E meridian; Fig. 7 in Stramma and Lutjeharms 1997). When seasonality in the latitude of the STF is considered (You 1997), this northward position in austral winter is even more anomalous. Therefore, the formation of SAMW around the 60°E meridian may well be associated with an anomalously northward position of the subantarctic zone so that an anomalous circulation may be implicit in formation of significant quantities of SAMW at this longitude.

The output of the Fine Resolution Antarctic Model (FRAM) was studied to ascertain a timescale for SAMW to reach the retroflection from its formation zone at 40°S, 60°E. Differences between the FRAM output and observations of the Agulhas Current System are discussed in detail by Lutjeharms and Webb (1995), but generally the comparison is good. Using the particle trajectory scheme described by Döös (1995), but on a single level rather than in three dimensions, particles were followed backward in time from the Agulhas retroflection region. A mean velocity field, derived from the 72 monthly datasets of the years 11–16 of the FRAM integration, was used. Particles were injected every 0.5° of longitude and every 0.25° latitude in the water at a depth of 400 m between 33° and 38°S, 15° and 25°E; this equated to approximately 400 particles. After eight years of tracing the particles backward in time, four of these particles were in the environment of 40°S, 60°E (Fig. 12). Of the injected particles, ~1% trace backward to 40°S, 60°E along a path that is entirely consistent with the compact anticyclonic gyre described by Stramma and Lutjeharms (1997). The number of particles or amount of water traced back is likely to be an underestimate because of the unrealistic way that the Agulhas Current System is fed in FRAM. In FRAM the narrow East Madagascar Current is not well resolved and does not retroflect south of Madagascar, but rather contributes to the Agulhas Current (Lutjeharms 1996). Thus more of the traced particles will originate in the East Madagascar Current than are likely in reality.


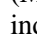
Although the amount of water that has been traced back to ~40°S, 60°E is likely to be an underestimate, this particle tracing exercise has given confirmation of a route in the southwest Indian Ocean subgyre and an associated timescale of eight years for water at ~40°S, 60°E to recirculate into the Agulhas retroflection. Given the shortcomings of using mean fields from FRAM to perform this aging task, then this 8-yr age can probably be believed to within a factor of 2.

8. Discussion

The thrust of this paper thus far has been to present a consistent sequence of events to explain the occurrence of Ring 1. There is other evidence in the observations of Ring 1 that reinforce this thesis and preclude other theses that have been put

forth. These will be presented together with some discussion of the implications of the implications of such as Ring 1.

Azimuthal velocities at 200 m in Ring 1 and Ring 2 were similar to one another and to other Agulhas rings ([Olson and Evans 1986](#)). In contrast to this the maximum velocity in a Brazil–Falklands (Malvinas) confluence ring which was 2–3 months old and had undergone wintertime modification of its surface waters was 35 cm s^{-1} ([Gordon 1989](#)), almost half that observed in Ring 1. Therefore, the velocity structure of Ring 1 precluded it from having been spawned anywhere other than the fast moving Agulhas retroflection.

As well as mapping the path of Ring 1, the satellite data used in this study held other information about the origin of the ring. There were two indicators from the altimeter and radiometer data collected after 14 April 1992 (i.e., during the *ERS-1* 35-day repeat) that confirmed that the Agulhas retroflection was the region of genesis of Ring 1. First, the magnitude of the sea surface height anomaly associated with Ring 1 in cycle 1 of the *ERS-1* 35-day repeat was greater than 50 cm ([Fig. 2i](#) ). Agulhas rings traced across the South Atlantic using satellite altimetry data decreased exponentially in height from in excess of 40 cm near the retroflection to about 10% of their original amplitude as they approached 40°W ([Byrne et al. 1995](#)). The height anomaly associated with Ring 1 was therefore comparable to other Agulhas rings detected in the region, and too high to have come from anywhere else. For comparison, recently spawned anticyclonic Brazil–Falklands (Malvinas) confluence rings had dynamic height anomalies of 20 and 27 dyn cm ([Gordon 1989](#)). Therefore a Brazil–Falklands (Malvinas) confluence origin for Ring 1, as suggested by [Smythe-Wright et al. \(1996\)](#), is extremely unlikely. The second indicator was depicted in [Fig. 4](#)  where Ring 1 was evident in both the altimetry and the ATSR data in August 1992. This indicated that the ring was less than one year old because its elevated sea surface temperature signal had not yet been destroyed by overwintering. This would require Ring 1 to travel at a minimum speed of 3 cm s^{-1} westward if it were formed at the Agulhas retroflection, as opposed to a minimum speed of 26 cm s^{-1} eastward if the ring had travelled from the Brazil–Falklands (Malvinas) confluence since the preceding winter. A speed of 3 cm s^{-1} is reasonable for an Agulhas ring. A minimum eastward speed for a ring of 26 cm s^{-1} seems fast. Although the currents in the region could account for this speed, the eastward motion is contrary to the self-induced motion of an anticyclonic ring, and also the ring would be expected to be less intact if it had been buffeted by such fast currents for extended periods of time. Most rings formed in the world's oceans have a limited life span because they are destroyed or reabsorbed by their parent current ([Olson 1991](#)). Agulhas rings have a peculiarly long lifetime because they are injected into a quiescent eastern ocean basin where the mean flow and the self-induced motion of the ring combine to move the ring westward away from the retroflection. This reinforces the unlikelihood of a Brazil–Falklands (Malvinas) confluence origin for Ring 1.

Ring 1 was traced for over a year (16 months) from when it was spawned to when it was sampled on WOCE Cruise A11. In addition to tracing the water in the southwest Indian Ocean in FRAM, this gives an age of the water sampled within Ring 1 of around 5–17 years. The homogeneous water at the core of Ring 1 was given an age of $4.16 \text{ years} \pm 4 \text{ months}$ from the CFCs measured on A11 ([Smythe-Wright et al. 1996](#)). This CFC mixing age for the water at the core of Ring 1 is within the age range given for the water by tracing the feature in the satellite data and particle tracing in FRAM. The age of the water given from apparent oxygen utilization rates also coincides with the range of ages given by this tracing exercise.

Although [Smythe-Wright et al. \(1996\)](#) concluded that Ring 1 formed at the Brazil–Falklands (Malvinas) confluence, it should be noted that the hydrography of Ring 1 was also different from typical anticyclonic rings observed to have formed at the Brazil–Falklands (Malvinas) confluence ([Gordon 1989](#)). Like the typical Agulhas Current rings, these western South Atlantic rings also tend to be stratified with surface properties modified by winter cooling and θ – S properties very similar to those at the Agulhas retroflection. However, an anomalous Brazil–Falklands (Malvinas) confluence ring was sampled by [Tsuchiya et al. \(1994\)](#) on a 25°W meridional section. The ring had a core of SAMW that stretched from the bottom of the mixed layer to 800 m. Based on its core θ – S characteristics of 15°C , 35.5 psu the ring was concluded to have spawned at the Brazil–Falklands (Malvinas) confluence, as [Gordon \(1981\)](#) had found SAMW which matched these properties within the loop of the Brazil Current. This is consistent with the definition of the thermostat associated with the SAMW varying from 14.5°C at 40°W , to 5.5°C at 80°W getting fresher, cooler, and denser to the east ([McCartney 1982](#)). So, the SAMW at the core of Ring 1 is too cool to have come from the Brazil–Falklands (Malvinas) confluence. High oxygen concentrations and low nutrient concentrations do not preclude Ring 1 from coming from the Agulhas retroflection; indeed, given the properties of the SAMW that feed the thermoclines of the Southern Ocean, Ring 1 is most likely to have come from the Agulhas retroflection. Furthermore, the analysis of the 13.6°C stad sampled by the ARC in the Agulhas retroflection (discussed in [section 6](#)) suggests that this stad came from the Indian Ocean rather than the South Atlantic Ocean, and discounted the possibility of that mode being formed by local modification. As this is the only time that such a stad has been observed in the Agulhas retroflection, it seems likely that the stad that made up the core of Ring 1 also came from the Indian Ocean. The results of this study imply that the presence of this water in the retroflection is a function of variability in the formation of SAMW, not only in its properties, but even whether it forms. This renewal may be associated with the meridional position of the fronts in the southwestern Indian Ocean.

A ring with a similar structure to Ring 1 was sampled in the Cape Basin in late 1993 during the third of the Benguela Source and Transport Program cruises (25 October 1993–9 November 1993). [Duncombe Rae et al. \(1996\)](#) concluded that this ring must have spawned at the Brazil–Falklands (Malvinas) confluence because it is so similar to Eddy B2-1 (Ring 1),

which Smythe-Wright et al. (1996) concluded to have formed at the western boundary of the South Atlantic. This study has demonstrated that it is much more likely that Ring 1 formed at the Agulhas retroflection, and similar arguments apply to Eddy B3-1. Preliminary analysis of altimetry data indicated that Eddy B3-1 had a sea surface height anomaly in excess of 30 cm associated with it, too large to have come from anywhere else other than the Agulhas retroflection.

Another ring (R3), documented by Arhan et al. (1999), had a very similar core structure to Ring 1 and was traced back to the Agulhas retroflection where it formed in May 1993. This ring was observed in the Angola Basin (north of the Walvis Ridge) as part of WOCE Hydrographic section A14. That three such anomalous rings were seen for the first time in the South Atlantic within two years of one another suggests that the stratification within the Agulhas retroflection varies and a component of this variability is interannual.

Variability in the water types (including SAMW) that enter the Agulhas retroflection has implications for the variability of the stratification of the water that makes up the interocean transport between the south Indian and the South Atlantic Oceans. This transport constitutes the warm water return path of the thermohaline circulation. When this $\sim 13^{\circ}\text{C}$ SAMW was observed in the retroflection by the Agulhas Retroflection Cruise, it was noted that the thermostat represented a positive salinity anomaly relative to the water flowing into the retroflection at the same potential temperature (Gordon et al. 1987). This positive salinity anomaly would give higher heat and salt content of the water relative to the input water at the same potential density. It therefore appears that an excess of this type of SAMW in the retroflection will enhance the flux of heat and salt from the south Indian to the South Atlantic Ocean in that potential density layer. The scheme that linked the warm water and cold water return paths by exchange in the subantarctic Indian Ocean had 4 Sv of Atlantic Ocean water converted to 11°C SAMW at 80°E , which then folds into the subtropical Indian Ocean (Gordon et al. 1992). The formation of 13°C SAMW at around 60°E short circuits the recirculation of the Atlantic Ocean water in the south Indian Ocean and will account for some of the warming required to convert the South Atlantic Ocean water to south Indian Ocean water in the south Indian Ocean subtropical gyre in the Gordon et al. (1992) model.

Acknowledgments

Our thanks go to Matthew Jones for furnishing us with the radiometer data. Thanks also to Peter Saunders and Brian King for providing us with the A11 data. Thanks to David Stevens for his assistance with particle tracking in FRAM. Thanks also to Arnold Gordon for drawing our attention to station 60 on the Agulhas Retroflection Cruise, and for his insightful discussion. This work was supported by a NERC UK WOCE special topic PhD studentship.

REFERENCES

- Arhan, M., H. Mercier, and J. R. E. Lutjeharms, 1999: The disparate evolution of three Agulhas rings in the South Atlantic Ocean. *J. Geophys. Res.*, in press..
- Byrne, D. A., A. L. Gordon, and W. F. Haxby, 1995: Agulhas eddies: A synoptic view using Geosat ERM data. *J. Phys. Oceanogr.*, **25**, 902–917. [Find this article online](#)
- Cartwright, D. E., and R. D. Ray, 1990: Oceanic tides from Geosat altimetry. *J. Geophys. Res.*, **95**, 3069–3090..
- Cheney, R. E., J. G. Marsh, and B. D. Beckly, 1983: Global mesoscale variability from collinear tracks of SEASAT altimeter data. *J. Geophys. Res.*, **88**, 4343–4354..
- Döös, K., 1995: Interocean exchange of water masses. *J. Geophys. Res.*, **100**, 13 499–13 514..
- Duncan, C. P., 1968: An eddy in the subtropical convergence southwest of South Africa. *J. Geophys. Res.*, **73**, 531–534..
- Duncombe Rae, C. M., 1991: Agulhas Retroflection rings in the South Atlantic Ocean: An overview. *S. Afr. J. Mar. Sci.*, **11**, 327–344..
- , S. L. Garzoli, and A. L. Gordon, 1996: The eddy field of the South East Atlantic Ocean: A statistical census from the Benguela Sources and Transport Project. *J. Geophys. Res.*, **101**, 11 949–11 964..
- Feron, R. C. V., W. P. M. De Ruijter, and D. Oskam, 1992: Ring shedding in the Agulhas Current System. *J. Geophys. Res.*, **97**, 9467–9477..
- Fine, R. A., 1993: Circulation of Antarctic Intermediate Water in the South Indian Ocean. *Deep-Sea Res.*, **40**, 2021–2042..
- , M. J. Warner, and R. F. Weiss, 1988: Water mass modification at the Agulhas Retroflection: Chlorofluoromethane studies. *Deep-Sea Res.*, **35**, 311–332..

Forrester, T. N., and P. G. Challenor, 1995: Validation of ATSR sea surface temperature in the Faroes region. *Int. J. Remote Sens.*, **16**, 2741–2753..

Goni, G. J., S. L. Garzoli, A. J. Roubicek, D. B. Olson, and O. B. Brown, 1997: Agulhas ring dynamics from TOPEX/POSEIDON altimeter data. *J. Mar. Res.*, **55**, 861–883..

Gordon, A. L., 1981: South Atlantic thermocline ventilation. *Deep-Sea Res.*, **28**, 1239–1264..

—, 1989: Brazil–Malvinas Confluence-1984. *Deep-Sea Res.*, **36**, 359–384..

—, and W. F. Haxby, 1990: Agulhas eddies invade the South Atlantic: Evidence from Geosat altimeter and shipboard conductivity–temperature–depth survey. *J. Geophys. Res.*, **95**, 3117–3125..

—, J. R. E. Lutjeharms, and M. L. Gründlingh, 1987: Stratification and circulation at the Agulhas Retroflection. *Deep-Sea Res.*, **34**, 565–599..

—, R. F. Weiss, W. M. Smethie, and M. J. Warner, 1992: Thermocline and intermediate water communication between the South Atlantic and South Indian Ocean. *J. Geophys. Res.*, **97**, 7223–7240..

Hernandez, F., P.-Y. LeTraon, and R. Morrow, 1995: Mapping mesoscale variability of the Azores Current using TOPEX/POSEIDON and ERS 1 altimetry, together with hydrographic and Lagrangian measurements. *J. Geophys. Res.*, **100**, 24 995–25 006..

Jones, M. S., M. A. Saunders, and T. H. Guymer, 1996: Global remnant cloud contamination in the ATSR data: Source and removal. *J. Geophys. Res.*, **101**, 12 141–12 147..

Lutjeharms, J. R. E., 1996: The exchange of water between the South Indian and South Atlantic Oceans. *The South Atlantic: Present and Past Circulation*, G. Wefer et al., Eds., Springer-Verlag, 125–162..

—, and R. C. van Ballegooyen, 1988: The retroflection of the Agulhas Current. *J. Phys. Oceanogr.*, **18**, 1570–1583.. [Find this article online](#)

—, and D. J. Webb, 1995: Modelling the Agulhas Current system with FRAM (Fine Resolution Antarctic Model). *Deep-Sea Res.*, **42**, 523–551..

Macdonald, A. L., and C. Wunsch, 1996: An estimate of global ocean circulation and heat fluxes. *Nature*, **382**, 436–439..

McCartney, M. S., 1977: SubAntarctic mode water. *A Voyage of Discovery, George Deacon 70th Anniversary Volume*, M. Angel, Ed., Pergamon, 103–119..

—, 1982: The subtropical recirculation of Mode Waters. *J. Mar. Res.*, **40**, 427–463..

McDonagh, E. L., 1997: Observations of mesoscale features in the South Atlantic and South Indian Oceans. Ph.D. thesis, University of East Anglia, Norwich, United Kingdom, 236 pp. [Available from School of Environmental Sciences, University of East Anglia, Norwich NR4 7TJ, United Kingdom.]

Mey, R. D., N. D. Walker, and M. R. Jury, 1990: Surface heat fluxes and marine boundary layer modification in the Agulhas Retroflection Region. *J. Geophys. Res.*, **95**, 15 997–16 015..

Olson, D. B., 1991: Rings in the ocean. *Ann. Rev. Earth Planet. Sci.*, **19**, 283–311..

—, and R. H. Evans, 1986: Rings of the Agulhas Current. *Deep-Sea Res.*, **33**, 27–42..

Saunders, P. M., and B. A. King, 1995: Bottom currents derived from a shipborne ADCP on WOCE Cruise A11 in the South Atlantic. *J. Phys. Oceanogr.*, **25**, 329–347.. [Find this article online](#)

—, and Coauthors, 1993: RRS Discovery Cruise 199, 22 December 1992–01 February 1993, WOCE A11 in the South Atlantic. IOSDL Cruise Rep. 234, Institute of Oceanographic Sciences Deacon Laboratory, Southampton, United Kingdom, 69 pp. [Available from Southampton Oceanography Centre, Empress Dock, Southampton, SO14 3ZH, United Kingdom.]

Schmitz, W. J., 1995: On the interbasin-scale thermohaline circulation. *Rev. Geophys.*, **33**, 151–173..

Smythe-Wright, D., A. L. Gordon, P. Chapman, and M. S. Jones, 1996: CFC-113 shows Brazil Eddy crossing the South Atlantic to the Agulhas Retroflection Region. *J. Geophys. Res.*, **101**, 885–895..

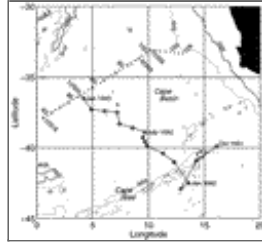
Stramma, L., and J. R. E. Lutjeharms, 1997: The flow field of the subtropical gyre of the South Indian Ocean. *J. Geophys. Res.*, **102**, 5513–5530..

Tsuchiya, M., L. D. Talley, and M. S. McCartney, 1994: Water-mass distributions in the western South Atlantic: A section from South Georgia Island (45S) northward across the equator. *J. Mar. Res.*, **52**, 55–81..

van Ballegooyen, R. C., M. L. Gründlingh, and J. R. E. Lutjeharms, 1994: Eddy fluxes of heat and salt from the southwest Indian Ocean into the southeast Atlantic Ocean: A case study. *J. Geophys. Res.*, **99**, 14 053–14 070..

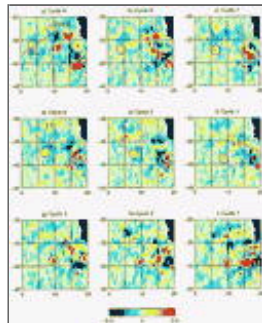
You, Y., 1997: Seasonal variations of thermocline circulation and ventilation in the Indian Ocean. *J. Geophys. Res.*, **102**, 10 391–10 422..

Figures



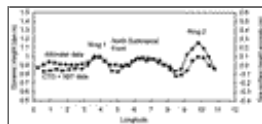
[Click on thumbnail for full-sized image.](#)

Fig. 1. The crossed circles indicate 16 monthly average positions of Ring 1, from when it was spawned at the Agulhas retroflection in October 1991 to when it was sampled on A11 in January 1993, as deduced from satellite data. Positions of XBT launches (crosses) and CTD stations (circles) in the Cape Basin completed during January 1993 as part of WOCE one-time hydrographic section A11 aboard RRS *Discovery*. The CTD stations are numbered 12316 to 12326. The XBT stations are numbered 82 to 109, with no XBT 107. The 2000 m (solid line) and 4000 m (dotted line) bathymetric contours are plotted.



[Click on thumbnail for full-sized image.](#)

Fig. 2. Sea surface height anomaly (in meters) from combined *ERS-1* 35-day repeat and TOPEX/POSEIDON data. Pictures are based on the 35-day repeat cycles of the *ERS-1* satellite. (a) Cycle 9, 19 Jan 1993–22 Feb 1993; (b) cycle 8, 15 Dec 1992–18 Jan 1993; (c) cycle 7, 10 Nov 1992–14 Dec 1992; (d) cycle 6, 6 Oct 1992–9 Nov 1992; and (e) cycle 5, 1 Sep 1992–5 Oct 1992. (f) Cycle 4, 28 Jul 1992–31 Aug 1992; (g) cycle 3, 23 Jun 1992–27 Jul 1992; (h) cycle 2, 19 May 1992–22 Jun 1992; and (i) cycle 1, 14 Apr 1992–18 May 1992. The portion of the A11 cruise track used to calculate the dynamic topography in [Fig. 3](#) is indicated in panel (a), as well as circles indicating the height anomalies associated with Ring 1 and Ring 2 in the cycle coincident with when they were sampled on A11. The position of Ring 1 is also indicated by a circle (which is not supposed to reflect size) in each of the other panels. In cycle 1 the sea surface height anomaly associated with Ring 1 is in excess of 50 cm.




[Click on thumbnail for full-sized image.](#)

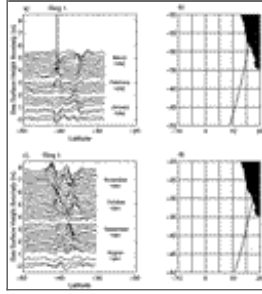
Fig. 3. Black symbols are dynamic height (in dynamic meters) at 100 db referenced to 760 db from CTD and XBT data combined. The gray symbols are altimetric sea surface height anomaly from a year long mean interpolated onto a line coincident with the A11 cruise track. Note that although the two scales are offset by an arbitrary amount, the range of each is 1 m. The major features in the section are labeled.





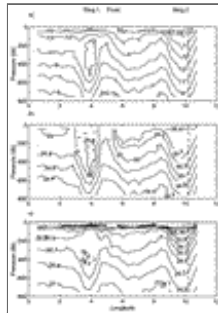
Click on thumbnail for full-sized image.

Fig. 4. Monthly average of sea surface temperature (in °C) from ATSR data for Aug 1992. The solid contour lines are 2°C apart. Additional dotted contour lines at 11.5°C and 12.5°C are included to improve the definition of the ring. The circle is the position of Ring 1 from the altimetry data for cycle 4 (28 Jul 1992 to 31 Aug 1992; [Fig. 2f](#) )




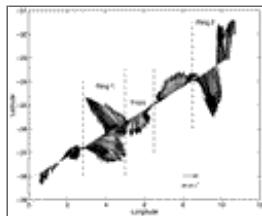
Click on thumbnail for full-sized image.

Fig. 5. (a) Sea surface height anomaly (in meters) along track 22, for *ERS-1* during the ice phase of the 3-day repeat (28 Dec 1991–30 Mar 1992), data for repeat cycles are offset by 0.2 m; (b) position of track 22 during the ice phase of the 3-day repeat; (c) sea surface height anomaly (in meters) along track 22, for *ERS-1* during the commissioning phase of the 3-day repeat (1 Aug 1991–12 Dec 1991), data for repeat cycles are offset by 0.2 m; (d) position of track 22 during the commissioning phase of the 3-day repeat.



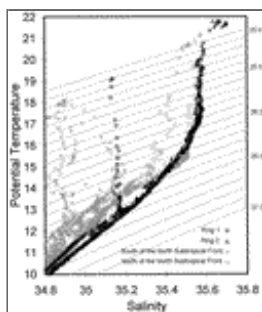
Click on thumbnail for full-sized image.

Fig. 6. Vertical section of (a) potential temperature (in °C), (b) salinity on the practical salinity scale, and (c) potential density. These sections use the XBT and CTD casts west of and including XBT 102 ([Fig. 1](#) ) . The positions of Ring 1, 2 and the front are indicated. The position of the dog leg in the cruise track is indicated by a dashed line in each of the sections.



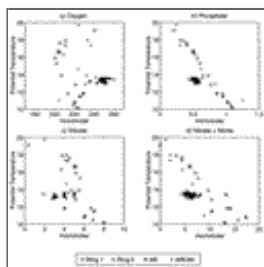
Click on thumbnail for full-sized image.

Fig. 7. Horizontal velocity vectors at 200 m from the ADCP. Data are averaged to 10 min and then smoothed using a 110-min running mean filter. ADCP data include on-station and underway data. Maximum velocity in Ring 1 is 58 cm s^{-1} and in Ring 2 is 60 cm s^{-1} .



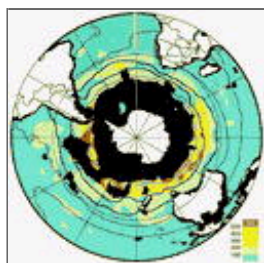
Click on thumbnail for full-sized image.

Fig. 8. Plot of θ - S for 2 db CTD data south of the front (gray crosses), north of the front (gray squares), within Ring 1 (black circles), within Ring 2 (black triangles). Potential temperature (in $^{\circ}\text{C}$), salinity (psu); σ_{θ} surfaces are shown between 25.0 and 27.0 at intervals of 0.1.



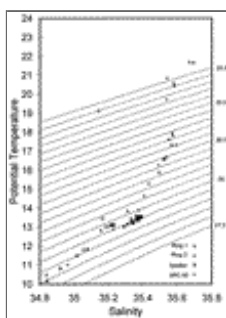
[Click on thumbnail for full-sized image.](#)

Fig. 9. Potential temperature ($^{\circ}\text{C}$) vs (a) dissolved oxygen, (b) phosphate, (c) silicate, and (d) nitrate plus nitrite concentration (micromolar or $\mu\text{mol l}^{-1}$). Circular symbols represent the station within Ring 1, \times symbols represent the two stations within Ring 2, star symbols represent the two stations sampled by the AB in 1963 within SAMW as it formed, and + symbols represent station 60 of the Agulhas Retroflection Cruise (ARC60), which sampled SAMW within the Agulhas retroflection in 1983.



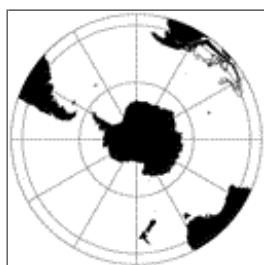
[Click on thumbnail for full-sized image.](#)

Fig. 10. Winter mixed layer depths (in meters), calculated using a 0.5°C criterion. Mixed layer temperatures are indicated by line contours at 5° , 10° , 15° , 20° , and 25°C . The 10° and 15°C mixed layer temperature contours are bold lines. Areas of absent data and points influenced by less than three data are black. Lines of latitude are at 0° , 30° , and 60°S .



[Click on thumbnail for full-sized image.](#)

Fig. 11. Plot of θ - S for bottle data within Ring 1 (circles), within Ring 2 (triangles), for the SAMW sampled by the AB in September 1963 in the south Indian Ocean around 40°S , 60°E (stars) and for the SAMW sampled at station 60 of the Agulhas Retroflection Cruise (ARC60) within the Agulhas retroflection (+ symbols): Potential temperature (in $^{\circ}\text{C}$), salinity (psu); σ_{θ} surfaces shown between 25.0 and 27.0 at intervals of 0.1.



[Click on thumbnail for full-sized image.](#)

Fig. 12. Trajectories of ~ 400 particles traced backwards in time from the Agulhas retroflection region using the mean velocity field from FRAM. The area south of South Africa was seeded every 0.25° of latitude between 38° and 33°S , and every 0.5° of longitude between 15° and 25°E . The particles have been traced for eight years. Lines of latitude are at 24° , 30° , and 60°S .

Corresponding author address: Elaine L. McDonagh, School of Environmental Sciences, University of East Anglia, Norwich NR4 7TJ, United Kingdom.

E-mail: e.mcdonagh@uea.ac.uk

top ▲



© 2008 American Meteorological Society [Privacy Policy and Disclaimer](#)

Headquarters: 45 Beacon Street Boston, MA 02108-3693

DC Office: 1120 G Street, NW, Suite 800 Washington DC, 20005-3826

amsinfo@ametsoc.org Phone: 617-227-2425 Fax: 617-742-8718

[Allen Press, Inc.](#) assists in the online publication of *AMS* journals.